

# Voltage band based improved particle swarm optimization technique for maximum power point tracking in solar photovoltaic system

T. Sudhakar Babu, K. Sangeetha, and N. Rajasekar

Citation: *J. Renewable Sustainable Energy* **8**, 013106 (2016); doi: 10.1063/1.4939531

View online: <http://dx.doi.org/10.1063/1.4939531>

View Table of Contents: <http://aip.scitation.org/toc/rse/8/1>

Published by the [American Institute of Physics](#)

---

---

## Voltage band based improved particle swarm optimization technique for maximum power point tracking in solar photovoltaic system

T. Sudhakar Babu, K. Sangeetha, and N. Rajasekar

*Solar Energy Research Centre, School of Electrical Engineering, VIT University, Vellore 632014, India*

(Received 18 June 2015; accepted 21 December 2015; published online 11 January 2016)

The extraction of maximum power from solar photovoltaic (PV) using Maximum Power Point Tracking (MPPT) methods is a promising research area in the recent past. Many methods including conventional methods, such as Hill Climbing and Incremental Conductance, and methods based on neural network, Fuzzy logic and bio-inspired algorithms, were proposed for MPPT application. However, all these methods suffer from drawbacks such as slower convergence, reduced power output, predominant steady state oscillations, larger memory requirement, and complex structure. Hence, in this paper an attempt is made to enhance existing Particle Swarm Optimization technique by emphasizing proper initial value selection. The key features of this method include the ability to track the global peak power accurately under partial shading conditions with almost zero steady state oscillations, faster dynamic response, and easy implementation. Simulations are carried out for different shading patterns and the results obtained are compared with existing methods. Further, simulation results are validated via experimental values. © 2016 AIP Publishing LLC. [<http://dx.doi.org/10.1063/1.4939531>]

### I. INTRODUCTION

Generation of electricity from solar energy has gained worldwide acceptance due to its abundant availability and eco-friendly nature.<sup>1</sup> However, power generation using solar energy still remains uncertain due to the following factors: poor energy conversion efficiency, high installation cost, and reduced power output under varying environmental conditions. Since the characteristics of solar PV being non-linear in nature, it imposes constraints on power generation. Therefore, to maximize the power output, Maximum Power Point Tracking (MPPT) algorithm becomes essential.<sup>2</sup>

Various MPPT algorithms<sup>3-5</sup> have been investigated and reported in the literature, and the most popular ones are Fractional Open Circuit Voltage,<sup>6-8</sup> Fractional Short Circuit Current,<sup>9-11</sup> Perturb and Observe (P&O),<sup>12-17</sup> Incremental Conductance (Inc. Cond.),<sup>18-22</sup> and Hill Climbing (HC) algorithm.<sup>23-26</sup> In fractional open circuit voltage and fractional short circuit current methods, tracking is based on an approximate linear relation between  $V_{mpp}$ ,  $V_{oc}$  and  $I_{mpp}$ ,  $I_{sc}$ , respectively.<sup>7</sup> Hence, exact value of Maximum Power Point (MPP) cannot be assured. The popular P&O method is based on perturbing the voltage or current by a small value based on the present and previous power values.<sup>20-23</sup> Regardless of its simple structure, the efficiency of the algorithm mainly depends on the tradeoff between the tracking speed and steady state oscillations in the region of MPP.<sup>15</sup> As an alternative to the P&O method, Incremental conductance algorithm is proposed where it operates on the principle of comparing ratios of incremental conductance with instantaneous conductance, and moreover, this method also has the similar disadvantage as that of P&O.<sup>20,21</sup>

Since conventional MPPT techniques may get trapped in any one of the local peaks instead of global peak under partial shading conditions, its power output lowers by a large extent. Hence, certain modifications were introduced in the conventional methods with the aim of

tracking the global maximum power point precisely even under change in environmental conditions. Among the many methods proposed, the most popular ones are a two stage approach: the Fibonacci line search method and DIRECT search algorithm.<sup>27–29</sup> In two stage methods, a wide search is performed in the first stage, while search space is fine tuned in the second stage so as to reach the peak power.<sup>27</sup> However, it fails to track the global peak under all conditions. Another interesting method for MPP tracking is the Fibonacci search method.<sup>28</sup> Like the two stage method, this one suffers from the inability to track MPP under all shading conditions. Another unique formulation combining the DIRECT search method with P&O algorithm was proposed for global MPP tracking.<sup>29</sup> Even though it is rendered effective, it is very complex, increasing the computational burden.

Realizing the above stated drawbacks, several researchers worked on applying Artificial Intelligence (AI) techniques like Neural Network (NN)<sup>30,31</sup> and Fuzzy Logic Control (FLC)<sup>32,33</sup> methods for better MPP tracking. However, these techniques require periodic training, enormous volume of data for training, computational complexity, and large memory capacity which makes them not feasible for MPPT applications. In the recent past, bio-inspired algorithms have drawn considerable attention of researchers for MPPT application as they ensure sufficient class of accuracy while dealing with non-linear, non-differentiable, and stochastic problems without involving excessive mathematical computations.<sup>34–36</sup> Further, these methods offer various advantages such as computational simplicity, easy implementation, and faster response. Among the evolutionary algorithms proposed, the Particle Swarm Optimization (PSO) method has gained popularity, and it is been widely used for solar MPPT as it provides faithful results. PSO is a search-based optimization technique and is based on the social behavior of flocks of birds, insects, or fishes. PSO is simple, easy to implement, system independent, highly adaptable, low computational burden, and fast converging. When a solar PV system is subjected to partial shading conditions, its I-V as well as P-V curves exhibit multimodal characteristics and the PSO method handles it efficiently.

However, in the PSO method, initial particle positions are randomly generated and particles are allowed to move in random directions until best solutions are reached, but increased number of particles and randomness in initial guess significantly deteriorate PSO performance in terms of larger computational time, momentary loss of power, and steady state oscillations.<sup>37,38</sup> Hence in order to maximize the search efficiency, it is necessary to ensure that the aforementioned drawbacks are nullified. Some authors proposed improved initialization procedures to enhance the performance of the conventional PSO method for Maximum Power Point Tracking. In the work of Refs. 39 and 37, the concept of reflective impedance<sup>29</sup> was used to locate the duty cycle limits. However, the duty cycle bounds obtained using this concept fail to restrict the duty cycle range to a smaller scale as it is purely based on assumptions. Due to this, the convergence to global peak takes longer time which reduces its search efficiency. In this work, a new methodology named Improved PSO is formulated for effective duty cycle initialization which in turn boosts up PSO with faster convergence, reduced steady state oscillations, and minimal power fluctuations. The underlying concept for the novel initialization procedure is the existence of a duty cycle within the voltage band limits where all the global MPPs lie.

Remaining section of the paper is organized as follows: Section II discusses PV modeling using single diode model and characteristics of partial shaded PV array. Section III deals with description about the proposed Improved Particle Swarm Optimization (IPSO) algorithm and its implementation. Simulation and experimental results are given in Section IV along with their comparison with other conventional methods. Finally, conclusions derived are presented in Section V.

## II. MODELING OF PV MODULE

### A. Single diode model

Generally, the nonlinear characteristics of solar cell are modelled with the help of single diode or double diode model. Single diode model is simple and moderately accurate. The practical single diode model is depicted in Fig. 1. It consists of a current source ( $I_{PV}$ ) connected in

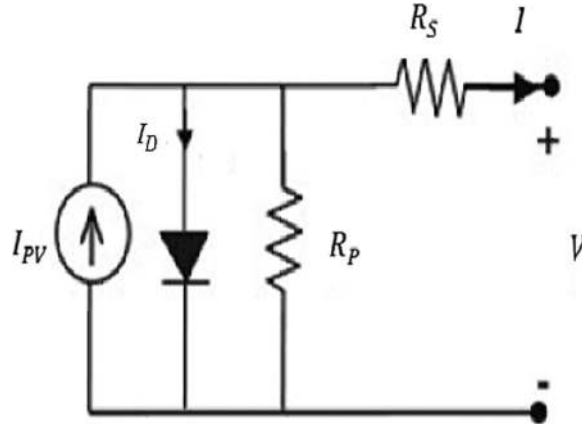


FIG. 1. Single diode model for PV modeling.

parallel with a diode, in addition to  $R_s$  and  $R_p$  which represent the voltage drop due to metal grid, contacts, and leakage losses.

The output current of solar PV module obtained according to this model can be formulated using Kirchoff's Current Law (KCL) and is given below

$$I = I_{pv} - I_D - \frac{V + IR_s}{R_p}, \quad (1)$$

where  $I_D$  is the diode current.

According to the ideal law, the ideal diode equation is given by

$$I_D = I_o (e^{V_D/aV_t} - 1), \quad (2)$$

where  $a$  is the ideality constant of diode and  $V_t$  is the thermal voltage.

At any temperature, the thermal voltage is defined by

$$V_t = N_s kT/q, \quad (3)$$

where  $k$  is the Boltzmann constant  $= 1.3805 \times 10^{-23}$  J/K,  $T$  is the cell temperature in Kelvin,  $q$  is the electron charge  $= 1.6 \times 10^{-19}$  C, and  $N_s$  is the number of cells in series.

To predict the model characteristics of solar PV accurately, Equations (4) and (5) presented in Ref. 41 are to be used. A detailed discussion on accurate modeling of series and parallel connected modules for partial shading condition is presented in Ref. 38.

$$V_{oc} = V_{ocn} + V_t \ln \left( \frac{G}{G_n} \right) + k_v dT + \alpha \log \left( \frac{G}{G_n} \right), \quad (4)$$

$$V_{mp} = V_{mpn} + V_t \ln \left( \frac{G}{G_n} \right) + k_v dT + \beta V_t \log \left( \frac{G}{G_n} \right). \quad (5)$$

From the above equations, it is evident that, to model solar PV characteristics using single diode model, computation of five parameters is essential. These values are identified using steps given in Ref. 41. For partial shading condition, Equation (1) needs to be modified by introducing  $N_{pp}$  and  $N_{ss}$  terms, i.e.,

$$I = N_{pp} \left\{ I_{PV} - I_o \left[ \exp \left( \frac{V + IR_s}{V_t N_{ss}} \right) - 1 \right] \right\} - \left( \frac{V + IR_s}{R_p} \right), \quad (6)$$

where  $N_{ss}$ ,  $N_{pp}$  are number of series and parallel connected PV modules.

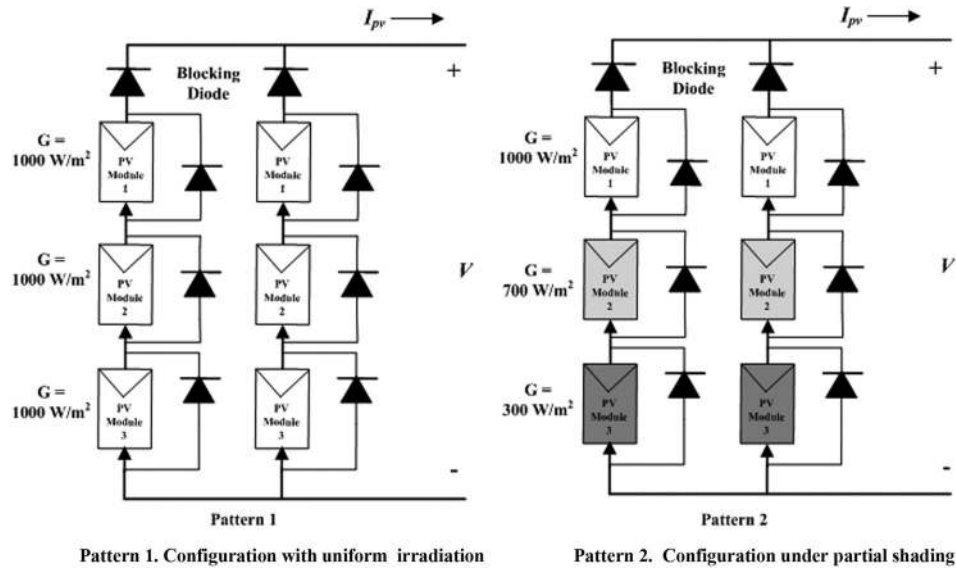


FIG. 2. 3S-2P PV system configuration.

**B. Partially shaded PV array characteristics**

To maximize the power output of solar PV modules, PV panels are connected in series-parallel arrangements. Blocking diodes and bypass diodes are used to prevent the reverse flow of current when strings are connected in parallel and to prevent hotspots in modules under partial shading conditions, respectively.<sup>42</sup> Partial shading occurs when the panels receive unequal insolation level due to the passing of clouds over the panels, shading caused by building or trees, etc. Depending on the shading pattern/level, the corresponding bypass diodes of the panels are activated which results in multiple power peaks. To demonstrate the effect of partial shading condition, PV array is constructed with three PV modules connected in series to form a string and two strings in parallel. The schematic of this configuration henceforth named as 3S-2P configuration is shown in Fig. 2 along with its I-V & P-V characteristics in Fig. 3.

Under uniform irradiation, say,  $G = 1000 \text{ W/m}^2$ , all the modules receive equal insolation and hence there exists a single maximum power point and it is marked as point “a” in P-V curve. Under this condition, the bypass diodes are reverse biased. However, when partial shading occurs, PV modules are exposed to different irradiation patterns which results in multiple power peaks. For instance, if “m” panels are shaded, there exists “m + 1” power peaks in the P-V characteristics. It is important to mention that the number of steps in the I-V characteristics and number of peaks in P-V characteristics are decided by the number of panels shaded. A

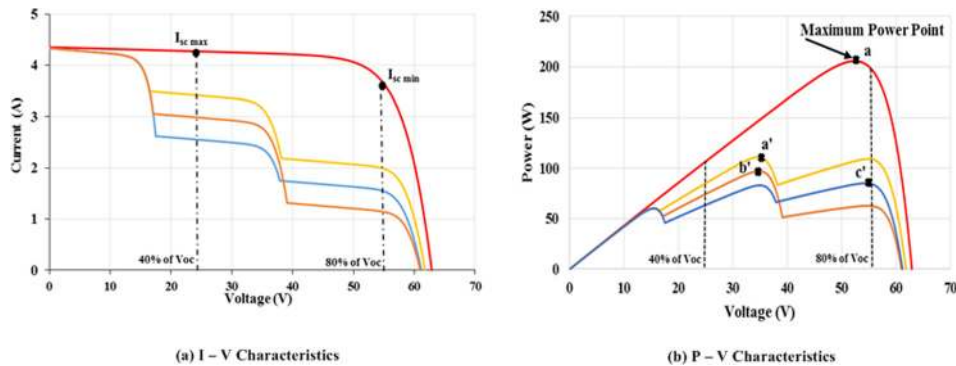


FIG. 3. I-V and P-V characteristics of 3S-2P configuration under uniform irradiation and partial shading conditions.

closer examination of the P-V curves corresponding to different shading patterns of S-36 panel shown in Fig. 3(b) confirms that all the global MPPs lie within a certain voltage range of 40%–80% of its  $V_{oc}$ . Further, when the search space is restricted within this range, then it is possible to speed up the search process and trapping of algorithm at local MPP can be avoided. Hence, this new voltage band is applied for PSO initialization and the new proposition is named as IPSO. Section III explains the details of the PSO method, the improved PSO method, and its problem formulation.

### III. OVERVIEW OF PSO AND PROPOSED METHOD

#### A. Overview of PSO algorithm

The PSO technique is one of the powerful methods for solving global optimization problems.<sup>43</sup> The PSO method has been studied by several researchers for MPPT application. The concept that underlines the PSO method is not obtained by the evolutionary mechanisms encountered in natural selection but by the intelligent social behavior of flocking of organisms, such as swarms of birds, fishes. In PSO, particles are randomly initialized at different positions and their positions are updated based on new velocity, previous positions, distance to  $pbest$ , and distance to  $gbest$ . This process is continued until termination criterion is reached.

The velocity and position of the particle are updated by using the following equation:

$$v_i^{t+1} = wv_i^t + c_1 \text{rand}() (pbest_i^t - x_i^t) + c_2 \text{rand}() (gbest_i^t - x_i^t), \quad (7)$$

$$x_i^{t+1} = x_i^t + v_i^{t+1}, \quad (8)$$

where  $w$  is the inertia weight factor,  $c_1$  and  $c_2$  are the learning coefficients,  $\text{rand}()$  is the random variable generated, and  $pbest$  and  $gbest$  are the particle best position and global best position of the particle, respectively.

The velocity and position updating of the PSO particle in search space are governed by Equations (7) and (8), and it can be graphically represented as shown in Fig. 4.

For better understanding, discussion on a popular conventional MPPT method namely, Hill Climbing method is presented. In the HC method, the duty cycle is periodically incremented with a fixed step size of  $\Delta d$  in the direction of increasing power and its direction is reversed

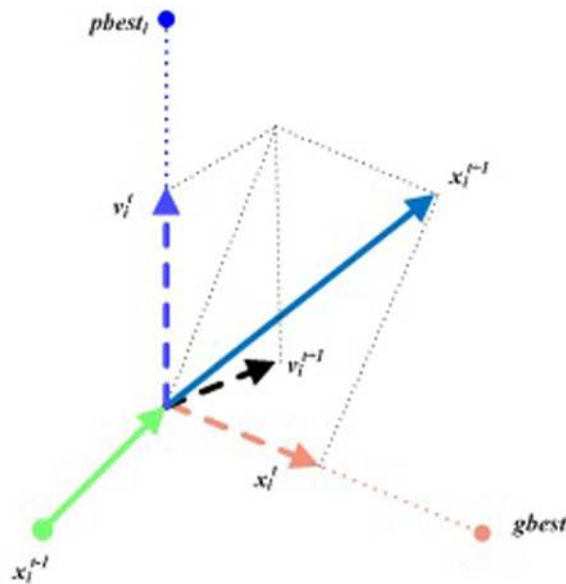


FIG. 4. Particle movement in the search space.

when it moves away from MPP. However, the method can be confused and track the MPP in the wrong direction,<sup>44</sup> when the change in PV power caused by change in irradiance is larger than the change in PV power as a function of the perturbation.

$$d_{present} = \begin{cases} d_{previous} + \Delta d & \text{if } P_{present} > P_{previous} \\ d_{previous} - \Delta d & \text{if } P_{present} < P_{previous} \end{cases} \quad (9)$$

The major drawbacks of the above conventional method are its deviation from maximum power point in case of rapidly changing conditions, slower convergence, and steady state oscillations around MPP which occurs due to fixed step size. However, these drawbacks are not present in case of the PSO method. Further, Equation (8) can be related with Equation (9) in such a way that each particle ( $x_i$ ) in PSO represents duty cycle of the converter and can be updated by applying PSO algorithm. One advantage with this approach is that duty cycle can be adjusted based on the particle position.

## B. Proposed improved PSO algorithm

Even though PSO possesses great computational power compared to conventional MPPT methods, its performance largely depends on initial value selection. In the conventional PSO method, initial values are randomly generated which results in the reduction of search efficiency.<sup>40</sup> If the initial duty cycle values are not confined within well defined limits, the algorithm requires increased number of iterations to converge to the global maximum, which deteriorates its performance. If the initial duty cycle boundaries are narrowed down, the PSO method can show improved efficiency guaranteeing faster convergence. At the same time, it has to be ensured that no global peak is left outside the band at any situation. Keeping the above factors in mind, a unique formulation based on the concept of voltage band is put forward for enhancing PSO performance for MPP tracking by defining the upper and lower bounds of duty cycle effectively.

In this initialization procedure, the voltage band accommodating all the global peaks irrespective of the irradiation pattern received by the PV array is utilized for MPPT. In order to confine the duty cycles within definite boundaries, P-V curves for different possible irradiation combinations ranging from 100 W/m<sup>2</sup> to 1000 W/m<sup>2</sup> were plotted for 3S-2P configuration. From the results, it was found that all the global peak values lie within a certain voltage range called as voltage band, and it can be expressed as a fraction of its open circuit voltage  $V_{oc}$  for any panel. For the panel under study S-36, this band is found to be between 40% and 80% of its  $V_{oc}$ . The above statement is confirmed via P-V characteristics presented in Fig. 3. The flowchart representing the IPSO method for MPP tracking is shown in Fig. 5.

## C. Problem formulation

The duty cycle limits namely,  $D_{min}$  and  $D_{max}$  are obtained from the voltage band by applying the principle of reflective impedance. The steps involved are given in detail below:

The search for global peak begins with initial set of  $N_p$  particles defined by

$$x_i^t = d_i^t = [d_1, d_2, \dots, d_{N_p}], \quad (10)$$

where  $t$  is the number of iteration.

The objective function of the proposed IPSO method is

$$F(x_i^k) > f(P_{besti}). \quad (11)$$

The above objective function focuses on maximizing the power output of the PV array by identifying an optimal duty cycle.

For a boost converter,

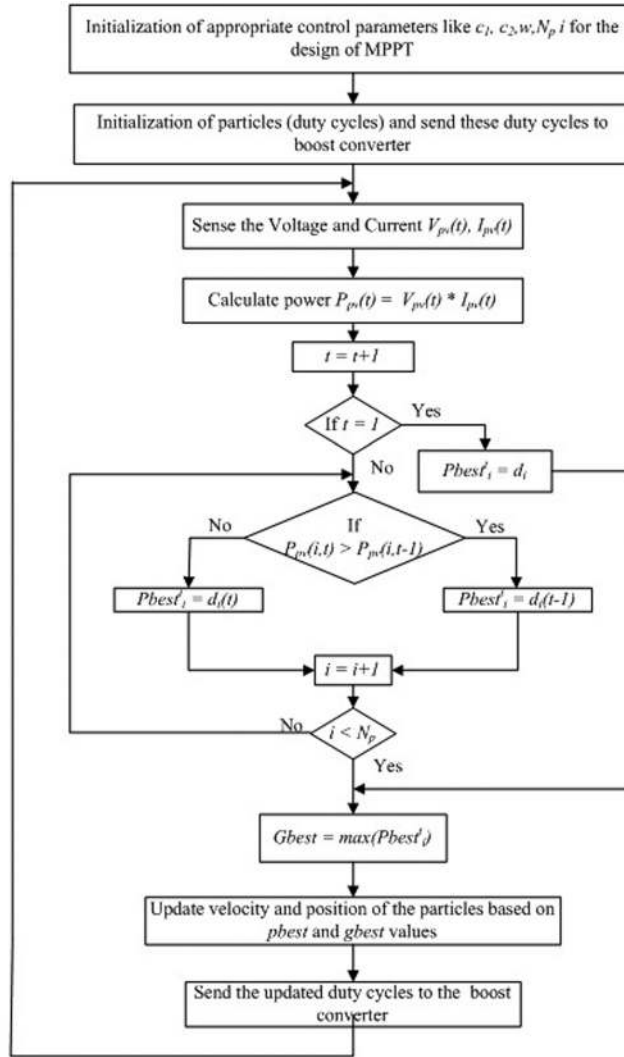


FIG. 5. Flowchart of IPSO algorithm.

$$R_{PV} = (1 - D)^2 * R_{load} * \eta_b. \tag{12}$$

Rearranging this equation, we get

$$D = \frac{\sqrt{R_{load} * \eta_b} - \sqrt{R_{PV}}}{\sqrt{R_{load} * \eta_b}}. \tag{13}$$

The minimum and maximum limits of duty cycle for the present study are computed using the following equations:<sup>38</sup>

$$D_{min} = \frac{\sqrt{R_{loadmin} * \eta_b} - \sqrt{R_{PVmin}}}{\sqrt{R_{loadmin} * \eta_b}}, \tag{14}$$

$$D_{max} = \frac{\sqrt{R_{loadmax} * \eta_b} - \sqrt{R_{PVmax}}}{\sqrt{R_{loadmax} * \eta_b}}, \tag{15}$$

where the minimum and maximum reflective impedances of the PV array  $R_{PVmin}$  and  $R_{PVmax}$ , respectively, can be found using the following formulae:

$$R_{PVmin} = \frac{V_{ocmin}}{I_{SCmax}} = \frac{40\% \text{ of } V_{oc}}{I_{SCmax}}, \tag{16}$$

$$R_{PVmax} = \frac{V_{ocmax}}{I_{SCmin}} = \frac{80\% \text{ of } V_{oc}}{I_{SCmin}}, \tag{17}$$

where  $\eta_b$  is the converter efficiency and  $R_{Lmin}$  and  $R_{Lmax}$  are the minimum and maximum values of the load resistance, respectively. The occurrence of partial shading is deducted by observing the difference in voltage and current using Equations (18) and (19). In the present work 0.1 and 0.2 values are chosen for current and voltage limits. Further, these values are arrived at based on the values of  $I_{MPP}$  and  $V_{MPP}$ , i.e., 90% and 80% of  $I_{sc}$  and  $V_{oc}$ .

$$\frac{I_{d3} - I_{d2}}{I_{d3}} \geq 0.1, \tag{18}$$

$$\frac{V_{d1} - V_{d2}}{V_{d1}} \geq 0.2. \tag{19}$$

#### IV. SIMULATION AND EXPERIMENTAL RESULTS

In order to demonstrate the effectiveness of the proposed method, the obtained results are compared with that of the conventional HC and PSO methods. The system configuration comprises a PV array, DC-DC boost converter, MPPT controller, and voltage and current sensors, and it is shown in Fig. 6. MPPT controller is programmed with the proposed as well as other MPPT algorithms.

##### A. Simulation results

For simulation, a dedicated MATLAB/SIMULINK model is developed and IPSO algorithm along with the other two, i.e., HC and PSO, methods are tested. DC-DC boost converter is operated at a switching frequency of 10 kHz with L and C values of 700  $\mu$ H mH and 100  $\mu$ F, respectively. The boost converter is operated in Continuous Conduction Mode and the algorithms are tested for two different conditions: (1) Uniform irradiation and (2) Partial shading. Under uniform irradiation, the irradiation and temperature are kept constant. During partial shaded condition, the irradiation received by PV modules is different while the temperature maintained constant. During simulation, enough care is taken to ensure that all the three methods are compared at the same instant with the same operating conditions. This is essential since the efficiency of the proposed method is judged based on this comparison. In this work, the

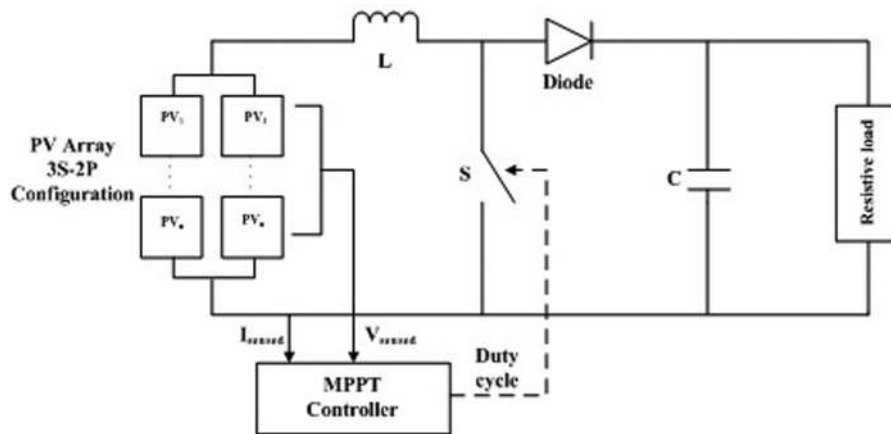


FIG. 6. System configuration.

PSO and IPSO parameters are taken from the existing literature and are fine-tuned to suit shaded conditions are presented in Table I.

**1. Uniform irradiation condition**

Simulation results showing voltage, current, and tracked power waveforms corresponding to uniform irradiation applying HC, PSO, and IPSO methods are presented in Fig. 7(a). To simulate uniform irradiation pattern, irradiation received by all panels in 3S-2P configuration is set to 1000 W/m<sup>2</sup>. For the HC method, a fixed perturbation step of 0.02 is taken. The step size is chosen considering the tradeoff between the steady state oscillations and tracking speed. From Fig. 7(a), it is clearly evident that steady state oscillations persist around MPP for the HC method. Further, the HC method converges to maximum power of 200 W taking 6 s to reach steady state. The PSO method also converges to global optima of 200 W with a convergence time of 9 s. In case of the IPSO algorithm, three initial duty cycles computed using Equations (13) and (14) are sent to the boost converter. These values are updated applying the IPSO algorithm until global peak is reached. The proposed IPSO method converges to MPP with a power of 200 W with a convergence time of 5 s. From the results, it is clear that IPSO method takes lesser time for settling and stays at MPP with almost zero steady state oscillations.

**2. Partial shading condition**

To assimilate partial shading effect in 3S-2P configuration, the lowermost panels are set to irradiation level of 700 W/m<sup>2</sup> and 300 W/m<sup>2</sup>, and the remaining panel is maintained with an irradiation of 1000 W/m<sup>2</sup>. Simulation results are taken for the HC, PSO, and IPSO methods considering partial shading conditions and are shown in Fig. 7(b). The HC method reaches local MPP having power value slightly lower than 65 W failing to locate the global peak with a lower convergence time of nearly 4 s due to its initialization being closer to the local peak. The PSO method manages to track the global peak whose power value is 106 W and takes a convergence time of 9 s, whereas the IPSO method converges to same global power within shorter time duration of 5 s.

In case of HC, oscillations are predominant at the region of MPP. In comparison with the HC algorithm, PSO provides better tracking when sudden change in irradiation occurs. However, the tracking takes more time especially during partial shaded conditions. The IPSO algorithm provides better dynamic response by initializing three duty cycles and it settles to global peak without any oscillations.

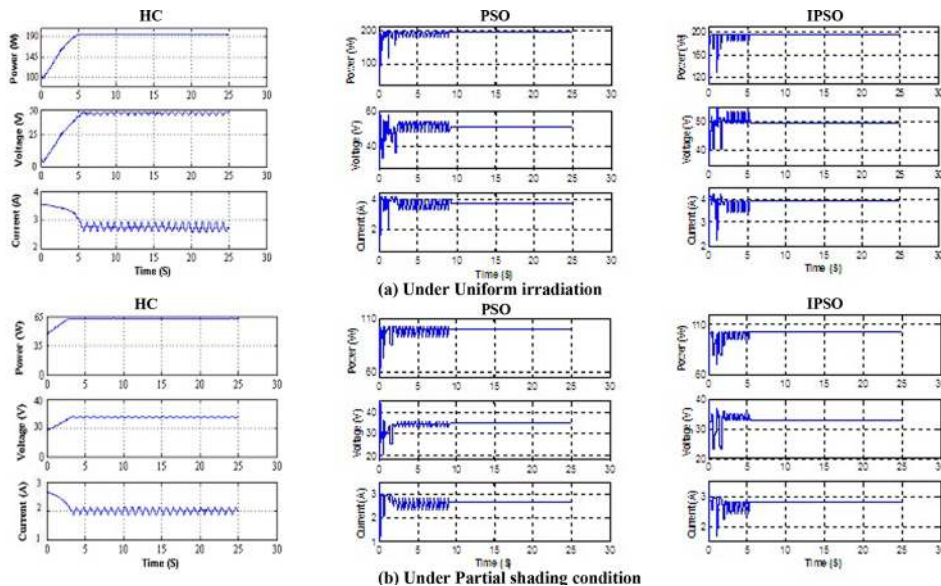


FIG. 7. Change in power, voltage, and current of the PV system for HC, PSO, and IPSO methods.

TABLE I. PSO and IPSO parameter values.

Parameter	PSO	IPSO
w	0.9	0.4
C <sub>1</sub>	1.1	1.4
C <sub>2</sub>	1.2	1.8

## B. Experimental results

In order to confirm the simulation study, experimentations were carried out on 3S-2P configuration under uniform irradiation and partial shading conditions. A hardware prototype is built in the laboratory and tested. The prototype is presented in Fig. 8. The hardware setup comprises a boost converter with designed values of inductor ( $700 \mu\text{H}$ ), capacitor ( $1000 \mu\text{F}$ ), and a load resistance of  $50 \Omega$ . To drive the Insulated Gate Bipolar Transistor (IGBT), triggering pulses are generated and MPPT algorithms are programmed using low-cost Arduino microcontroller. With the developed hardware circuit, HC, PSO, and proposed IPSO algorithms are tested for uniform as well as partial shading conditions. The partial shading condition is achieved by covering the panels with layers of sheets and maintaining the irradiances of the panels at  $1000 \text{ W/m}^2$ ,  $700 \text{ W/m}^2$ , and  $300 \text{ W/m}^2$ , respectively.

### 1. Uniform irradiation condition

The recorded input voltage, input current, and output voltage waveforms for HC, PSO, and IPSO algorithm under this condition are shown in Fig. 9. From the results, it is clear that there exists good agreement between the simulated and experimental results. Further, it is noticed that, unlike simulation, steady state oscillations still persist at the region of MPP in case of HC as the duty cycle is perturbed by a fixed step size. The PSO method takes less time, say, 4 iterations, i.e., 50 s, to reach the global peak value compared to 80 s taken by HC algorithm. The time taken by PSO to settle is equivalently same as that of HC due to the random initialization. However, IPSO method takes just 3 iterations, i.e., 40 s, to reach the global peak value which is comparatively very much lower. The small discrepancy in the experimental results could be attributed to sensor value changes.

### 2. Partial shading condition

To further illustrate the capability of IPSO algorithm, shading patterns similar to simulation were set up and the results are obtained. Parameter initializations are maintained similar to that of uniform irradiation condition. The experimental waveforms for voltage and current corresponding to HC, PSO, and IPSO algorithm under this condition were noted down and presented

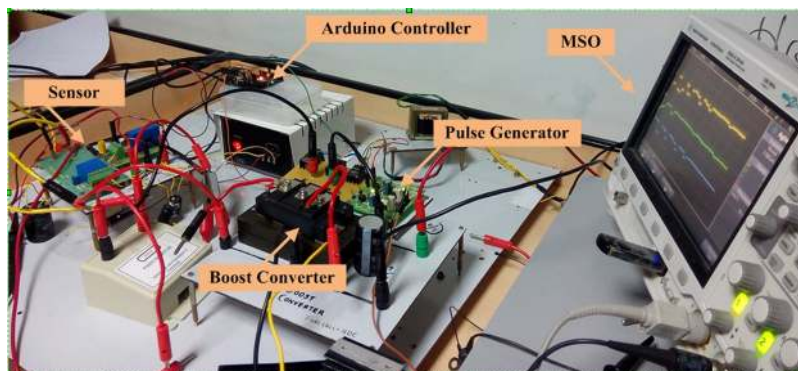


FIG. 8. Experimental test setup.

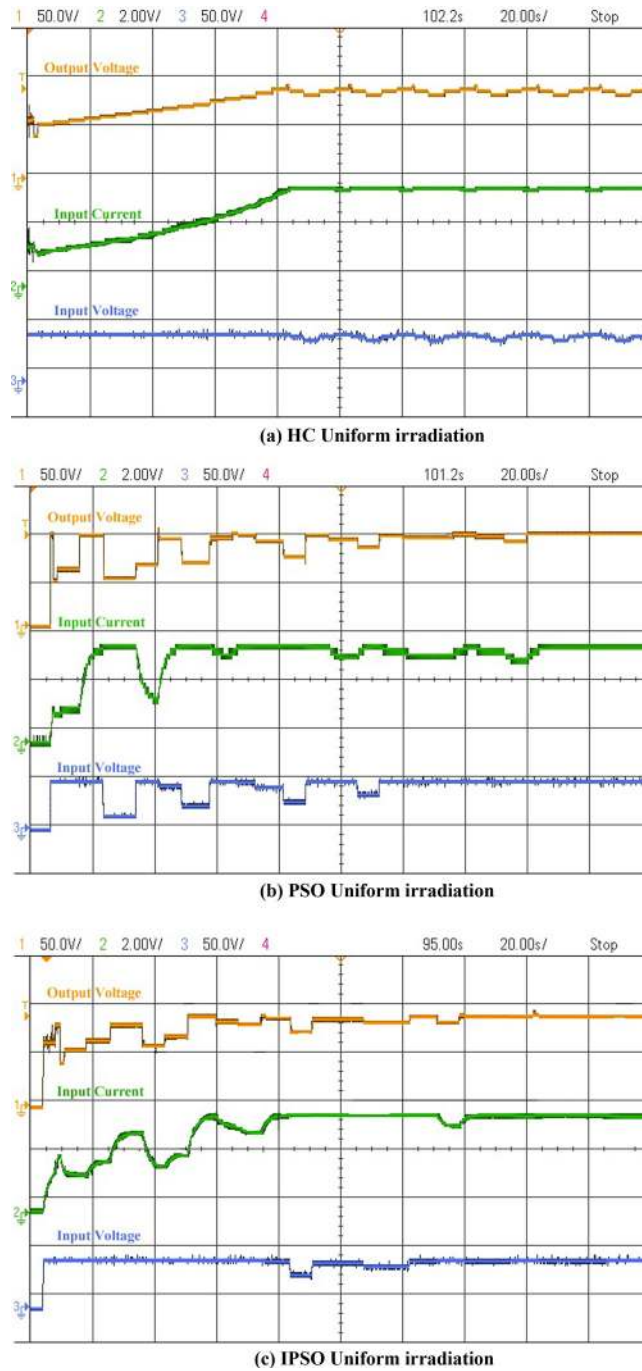


FIG. 9. Experimental results with 3S-2P configuration. (a) HC uniform irradiation, (b) PSO uniform irradiation, and (c) IPSO uniform irradiation.

in Fig. 10. It is obvious that using the HC method results in steady state oscillations at the vicinity of MPP regardless of change in atmospheric conditions. Moreover, it takes almost same time as that of uniform irradiation but it settles only at local peak utterly failing to reach its objective, i.e., convergence to global MPP under shaded conditions. PSO is able to locate the global peak, but with a settling time of 50 s, whereas IPSO converges precisely to the global maximum in just 2 iterations, thereby lowering down the tracking time to a great extent. Moreover, it is important to mention that the proposed IPSO method successfully attains global

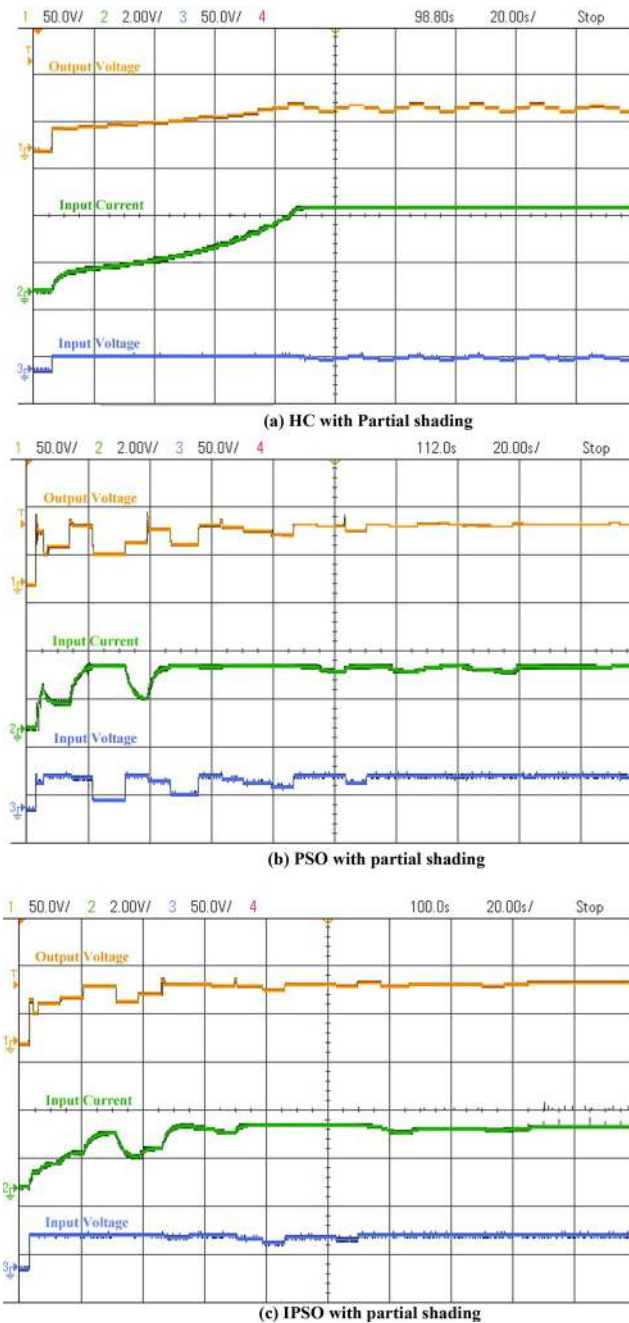


FIG. 10. Experimental results with 3S-2P configuration. (a) HC with partial shading, (b) PSO with partial shading, and (c) IPSO with partial shading.

MPP with zero steady state oscillations even under change in irradiation conditions due to its well defined initial duty cycle values accommodating global power peak attributing to good dynamic as well as steady state performances.

### C. Performance comparison of the proposed method with conventional methods

To extensively study the performance of the IPSO method under different shading conditions, the method is subjected to various shading patterns. Power value is recorded for the IPSO, PSO, and HC methods: the recorded values are compared against the maximum

TABLE II. Comparison of power output with different methods.

Shading patterns	PV array			PV array output			
	PV module 1	PV module 2	PV module 3	Actual $P_{mpp}$ $P_{mpp}$	HC $P_{mpp}$	PSO $P_{mpp}$	IPSO $P_{mpp}$
P1	1000	1000	1000	205.848	192.14	204.62	205.848
P2	800	600	900	130.445	128.1	129.24	130.21
P3	1000	500	800	110.843	45.61	109.89	110.71
P4	1000	600	400	85.129	83.45	84.84	85.124
P5	400	600	800	84.412	57.14	84.41	84.41
P6	200	600	900	82.299	55.14	81.66	82.299
P7	500	100	800	67.415	66.35	67.415	67.415
P8	300	500	700	66.556	39.45	65.91	66.567
P9	1000	400	200	60.243	41.35	60.11	60.241
P10	200	400	600	51.918	39.6	51.2	51.85

attainable power. Based on the results, a comparison table is arrived and presented. From Table II, it is clear that the performance of the proposed IPSO method is found to be excellent compared to the HC and PSO methods, in terms of power tracked. Further tracking speed, steady state oscillations, and the ability to accurately track global peak even under partial shading conditions are good for the proposed IPSO method.

## V. CONCLUSION

In this paper, an Improved Particle Swarm Optimization technique with an effective duty cycle initialization incorporating the idea of voltage band was presented. The proposed method along with Hill Climbing and PSO was tested through simulations and experimentation for uniform as well as partial shading conditions. Based on simulation and experimental results, the following conclusions were obtained. The IPSO method was found to have good tracking ability, with almost zero steady state oscillations, providing good tracking speed with ease in implementation under uniform as well as partial shaded conditions.

## NOMENCLATURE

$c_1$	Acceleration factor
$c_2$	Acceleration factor
$dT$	Difference in temperature
$G$	Irradiation
$G_n$	Nominal irradiation
$g_{best}$	Global best position
$I_D$	Diode current
$I_0$	Leakage current
$I_{mpp}$	Current at maximum power point
$I_{PV}$	Current source
$I_{sc}$	Short circuit current
$K$	Boltzmann constant
$K_v$	Voltage temperature coefficient
$N_s$	Number of cells in series
$N_{pp}$	Number of parallel PV modules
$N_{ss}$	Number of series PV modules
$p_{best}$	Personal best position
$q$	Electron charge

$R_p$	Parallel resistance
$R_s$	Series resistance
$R_o$	Equivalent output load resistance
$R_{in}$	Internal resistance of the PV module
$R_{Lmax}$	Maximum value of load at output
$R_{Lmin}$	Minimum value of load at output
$R_{PVmax}$	Maximum reflective impedance of PV array
$R_{PVmin}$	Minimum reflective impedance of PV array
$T$	Temperature
$V_D$	Diode voltage
$V_t$	Thermal voltage
$V_{mpn}$	Nominal maximum power point voltage at 1000 W/m <sup>2</sup>
$V_{mpp}$	Voltage at maximum power point
$V_{oc}$	Open circuit voltage
$V_{ocn}$	Nominal open circuit voltage at 1000 W/m <sup>2</sup>
$w$	Weight factor
$\eta_b$	Converter efficiency

- <sup>1</sup>M. A. Eltawil and Z. Zhao, "MPPT techniques for photovoltaic applications," *Renewable Sustainable Energy Rev.* **25**, 793–813 (2013).
- <sup>2</sup>A. R. Reisi, M. H. Moradi, and S. Jamsb, "Classification and comparison of maximum power point tracking techniques for photovoltaic system," *Renewable Sustainable Energy Rev.* **19**, 433–443 (2013).
- <sup>3</sup>T. Esmar, J. W. Kimball, P. T. Krein, P. L. Chapman, and P. Midya, "Dynamic maximum power point tracking of photovoltaic arrays using ripple correlation control," *IEEE Trans. Power Electron.* **21**, 1282–1291 (2006).
- <sup>4</sup>V. Salas, E. Olías, A. Barrado, and A. Lázaro, "Review of the maximum power point tracking algorithms for stand-alone photovoltaic systems," *Sol. Energy Mater. Sol. Cells* **90**, 1555–1578 (2006).
- <sup>5</sup>N. Rajasekar *et al.*, "Application of modified particle swarm optimization for maximum power point tracking under partial shading condition," *Energy Procedia* **61**, 2633–2639 (2014).
- <sup>6</sup>K. Kobayashi, H. Matsuo, and Y. Sekine, "A novel optimum operating point tracker of the solar cell power supply system," in *Proceedings of the 35th Annual IEEE Power Electronics Specialists Conference* (IEEE, 2004), pp. 2147–2151.
- <sup>7</sup>M. A. Masoum, H. Dehbonei, and E. F. Fuchs, "Theoretical and experimental analyses of photovoltaic systems with voltage and current-based maximum power point tracking," *IEEE Power Eng.* **22**, 62 (2002).
- <sup>8</sup>J. H. R. Enslin, M. S. Wolf, D. B. Snyman, and W. Swiegers, "Integrated photovoltaic maximum power point tracking converter," *IEEE Trans. Ind. Electron.* **44**, 769–773 (1997).
- <sup>9</sup>N. Mutoh, T. Matuo, K. Okada, and M. Sakai, "Prediction-data-based maximum power-point-tracking method for photovoltaic power generation systems," in *IEEE 33rd Annual 2002 Power Electronics Specialists Conference* (IEEE, 2002), Vol. 1483, pp. 1489–1494.
- <sup>10</sup>T. Noguchi, S. Togashi, and R. Nakamoto, "Short-current pulse-based maximum-power-point tracking method for multiple photovoltaic-and converter module system," *IEEE Trans. Ind. Electron.* **49**, 217–223 (2002).
- <sup>11</sup>N. Hyeong-Ju, L. Dong-Yun, and H. Dong-Seok, "An improved MPPT converter with current compensation method for small scaled PV-applications," in *IEEE 2002 28th Annual Conference Industrial Electronics Society IECON 02* (IEEE, 2002), Vol. 1112, pp. 1113–1118.
- <sup>12</sup>A. G. B. Moacyr, L. Galotto, L. P. Sampaio, and A. M. Guilherme, "Evaluation of the main MPPT techniques for photovoltaic applications," *IEEE Trans. Ind. Electron.* **60**, 1156–1167 (2013).
- <sup>13</sup>M. A. Elgendy and B. Zahawi, "Assessment of perturb and observe MPPT algorithm implementation techniques for PV pumping applications," *IEEE Trans. Sol. Energy* **3**, 21–33 (2012).
- <sup>14</sup>N. Femia, G. Petrone, G. Spagnuolo, and M. Vitelli, "Optimization of perturb and observe maximum power point tracking method," *IEEE Trans. Power Electron.* **20**, 963–973 (2005).
- <sup>15</sup>A. Pandey, N. Dasgupta, and A. K. Mukerjee, "High-performance algorithms for drift avoidance and fast tracking in solar MPPT system," *IEEE Trans. Energy Conserv.* **23**, 681 (2008).
- <sup>16</sup>A. K. Abdelsalam, A. M. Massoud, and S. Ahmed, "High-performance adaptive perturb and observe MPPT technique for photovoltaic-based microgrids," *IEEE Trans. Power Electron.* **26**, 1010–1021 (2011).
- <sup>17</sup>K. Hussein, I. Muta, T. Hoshino, and M. Osakada, "Maximum photovoltaic power tracking: An algorithm for rapidly changing atmosphere conditions," *IEEE Proc.* **142**, 59–64 (1995).
- <sup>18</sup>X. Zhu, D. Song, and M. Ma, "The simulation and design for MPPT of PV system based on incremental conductance method," in *2010 WASE International Conference Information Engineering (ICIE)* (2010), pp. 1314–1317.
- <sup>19</sup>L. Jae, B. Hyun Su, and C. Bo Hyung, "Advanced incremental conductance MPPT algorithm with a variable step size," in *12th International 2006 Power Electronics and Motion Control Conference, 2006 EPE-PEMC'06* (2006), pp. 603–607.
- <sup>20</sup>L. Jiyong and W. Honghua, "A novel stand-alone PV generation system based on variable step size INC MPPT and SVPWM control," in *IEEE 6th International Power Electronics and Motion Control Conference, 2009, IPEMC'09* (IEEE, 2009), pp. 2155–2160.
- <sup>21</sup>F. Liu, S. Duan, F. Liu, B. Liu, and Y. Kang, "A variable step size INC MPPT method for PV systems," *IEEE Trans. Ind. Electron.* **55**, 2622–2628 (2008).

- <sup>22</sup>M. S. Safari, "Simulation and hardware implementation of incremental conductance MPPT with direct control method using Cuk converter," *IEEE Trans. Ind. Electron.* **58**, 1154–1161 (2011).
- <sup>23</sup>P. J. Wolfs and L. Tang, "A single cell maximum power point tracking converter without a current sensor for high performance vehicle solar arrays," in *IEEE Power Electronics Specialists Conference* (IEEE, 2005), Vol. 20, pp. 165–171.
- <sup>24</sup>X. Weidong and W. G. Dunford, "A modified adaptive hill climbing MPPT method for photovoltaic power systems," in *IEEE Power Electronics Specialists Conference* (IEEE, 2005), Vol. 35, pp. 1957–1963.
- <sup>25</sup>M. Veerachary, T. Senjyu, and K. Uezato, "Maximum power point tracking control of IDB converter supplied PV system," in *IEE Proceedings of Electronics Power Applications* (IEEE, 2001), pp. 494–502.
- <sup>26</sup>O. Hashimoto, T. Shimizu, and G. Kimura, "A novel high performance utility interactive photovoltaic inverter system," in *Conference Record 2000 IEEE Industrial Applications Conference* (IEEE, 2000), pp. 2255–2260.
- <sup>27</sup>K. Kobayashi, I. Takano, and Y. Sawada, "A study on a two stage maximum power point tracking control of a photovoltaic system under partially shaded insolation conditions," in *IEEE Power Engineering Society General Meeting* (IEEE, 2003).
- <sup>28</sup>N. A. Ahmed and M. Miyatake, "A novel maximum power point tracking for photovoltaic applications under partially shaded insolation conditions," *Electr. Power Syst. Res.* **78**, 777–784 (2008).
- <sup>29</sup>T. L. Nguyen and K. S. Low, "A global maximum power point tracking scheme employing direct search algorithm for photovoltaic systems," *IEEE Trans. Ind. Electron.* **57**, 3456–3467 (2010).
- <sup>30</sup>K. Rai, N. D. Kaushika, B. Singh, and N. Agarwal, "Simulation model of ANN based maximum power point tracking controller for solar PV system," *Sol. Energy Mater. Sol. Cells* **95**, 773–778 (2011).
- <sup>31</sup>M. A. Islam and M. A. Kabir, "Neural network based maximum power point tracking of photovoltaic arrays," in *IEEE TENCON* (IEEE, 2011), Vol. 10, pp. 79–82.
- <sup>32</sup>N. Alajmi, K. H. Ahmed, S. J. Finney, and S. W. Williams, "Fuzzy logic-control approach of a modified hill-climbing method for maximum power point in microgrid standalone photovoltaic system," *IEEE Trans. Power Electron.* **26**, 1022–1030 (2011).
- <sup>33</sup>K. Syafaruddin and K. T. Hiyama, "Polar coordinated fuzzy controller based real time maximum power point control of photovoltaic system," *Renewable Energy* **34**, 2597–2606 (2009).
- <sup>34</sup>L. L. Jiang, D. L. Maskell, and J. C. Patra, "A novel ant colony optimization-based maximum power point tracking for photovoltaic systems under partially shaded conditions," *Energy Build.* **58**, 227–236 (2013).
- <sup>35</sup>Y. Shaiek, M. Ben Smida, A. Sakly, and M. F. Mimouni, "Comparison between conventional methods and GA approach for maximum power point tracking of shaded solar PV generators," *Sol. Energy* **90**, 107–122 (2013).
- <sup>36</sup>S. Subiyanto, A. Mohamed, and M. A. Hannan, "Intelligent maximum power point tracking for PV system using Hopfield neural network optimized fuzzy logic controller," *Energy Build.* **51**, 29–38 (2012).
- <sup>37</sup>I. R. Balasubramanian, S. I. Ganesan, and N. Chilakapati, "Impact of partial shading on the output power of PV systems under partial shading conditions," *IET Power Electron.* **7**(3), 657–666 (2014).
- <sup>38</sup>T. Sudhakar Babu, N. Rajasekar, and K. Sangeetha, "Modified particle swarm optimization technique based maximum power point tracking for uniform and under partial shading condition," *Appl. Soft Comput.* **34**, 613–624 (2015).
- <sup>39</sup>K. Ishaque and Z. Salam, "A deterministic particle swarm optimization maximum power point tracker for photovoltaic system under partial shading condition," *IEEE Trans. Ind. Electron.* **60**, 3195–3206 (2013).
- <sup>40</sup>R. Venugopalan, N. Krishnakumar, R. Sarjila, and N. Rajasekar, "Application of particle swarm optimization technique for the design of maximum power point tracking," *Adv. Mater. Res.* **768**, 47–56 (2013).
- <sup>41</sup>N. Rajasekar, K. Neeraja, and R. Venugopalan, "Bacterial foraging algorithm based solar PV parameter estimation," *Sol. Energy* **97**, 255–265 (2013).
- <sup>42</sup>M. A. M. Ramli *et al.*, "A modified differential evolution based maximum power point tracker for photovoltaic system under partial shading condition," *Energy Build.* **103**, 175–184 (2015).
- <sup>43</sup>J. Kennedy and R. Eberhart, "Particle swarm optimization," *IEEE Trans.* **4**, 1942–1948 (1995).
- <sup>44</sup>S. B. Kajer, "Evaluation of the hill climbing and the incremental conductance maximum power point trackers for photovoltaic power systems," *IEEE Trans. Energy Convers.* **27**, 922–929 (2012).